

Electronic Supplementary Information

High conductivity PEDOT:PSS through laser

micro-annealing: Mechanisms and application

J. G. Troughton,^{1, a)} N. Peillon,² A. Borbely,² J. Rodriguez-Pereira,^{3, 4} D. Pavlinak,⁴ J. M. Macak,^{3, 4} T. Djenizian,^{1, 5} and M. Ramuz^{1, b)}

¹⁾*Mines Saint-Etienne, Center CMP, Department FEL, F - 13541 Gardanne France*

²⁾*Mines Saint-Etienne, Univ Lyon, CNRS, UMR 5307 LGF, Center SMS, F - 42023 Saint-Etienne France*

³⁾*Center of Materials and Nanotechnologies, Faculty of Chemical Technology, University of Pardubice, Nám. Cs. Legií 565, 53002 Pardubice, Czech Republic*

⁴⁾*Central European Institute of Technology, Brno University of Technology, Purkyňova 123, Brno, Czech Republic*

⁵⁾*Al-Farabi Kazakh National University, Center of Physical-Chemical Methods of Research and Analysis, Almaty, Tole bi str., 96A, Kazakhstan*

^{a)}Electronic mail: joseph.troughton@dunelm.org.uk

^{b)}Electronic mail: ramuz@emse.fr

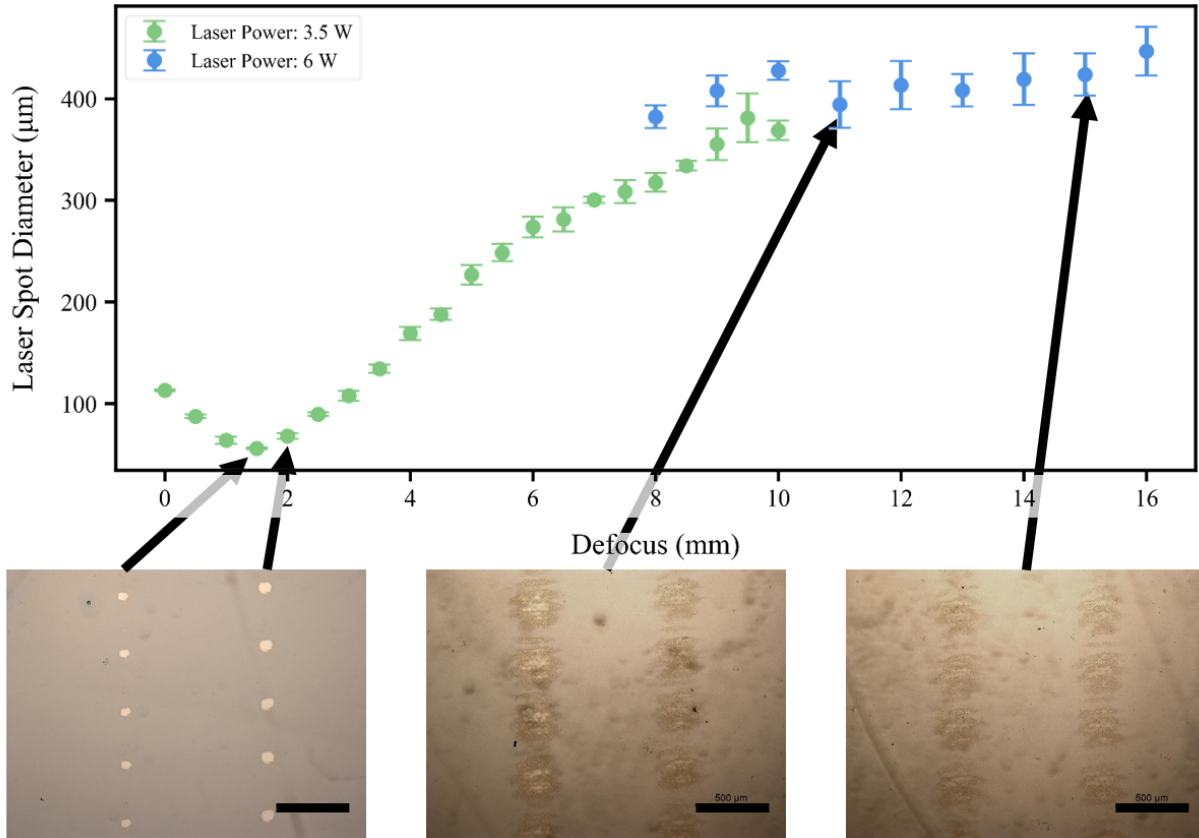


FIG. S1. Spot diameter with increasing focal height, or defocus, effectively describing the laser beam profile. Spot diameter measured using ImageJ software across 10 laser spots at each height, error bars represent one standard deviation in the measured size. Below a selection of optical images used to extract the spot sizes, scale bar is 500 µm.

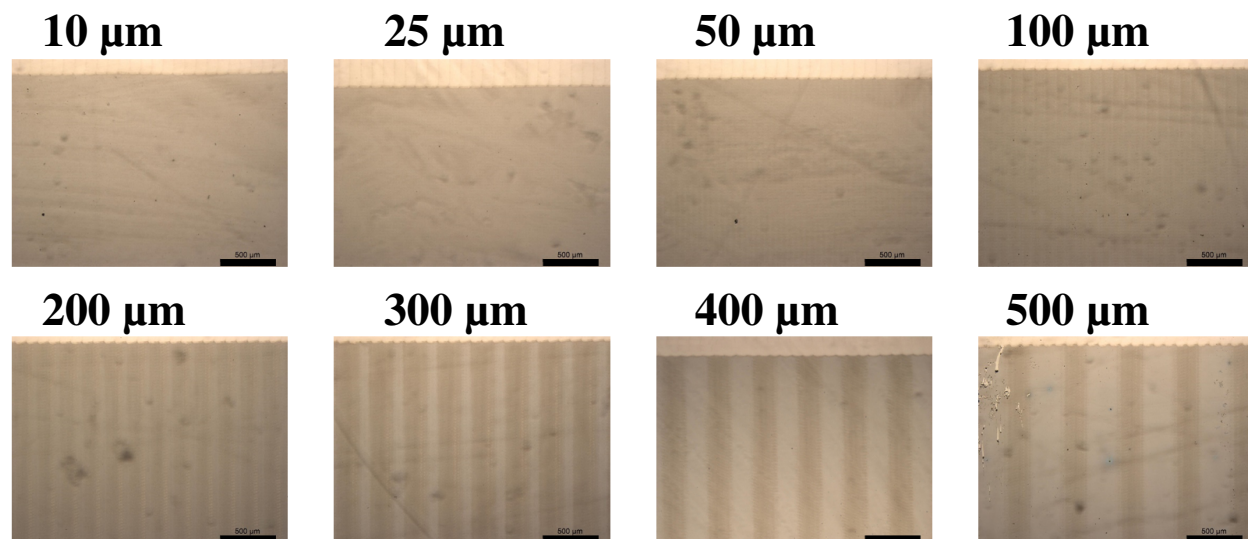


FIG. S2. Optical images of PEDOT:PSS with laser treatment at increasing line spacing, line spacing shown above each image, scale bar is 500 μm . The corresponding sheet resistances are shown in figure 2b of the main text. The laser lines become clearly visible above 200 μm , with the dark bands being the laser treated material, and the light bands being the untreated.

TABLE S1. Thickness, RMS Roughness, and Waviness of PEDOT:PSS films treated with increasing laser power. Data shown graphically in Figure 3A of the main text.

Laser Power (W)	0	0.5	1	1.5	2	2.5	2.6	2.7	2.8	2.9	3	3.2	3.4	3.6	3.8	4
Film Thickness (nm)	77.5	75.9	74.1	78.3	84.4	81.1	87.6	86.4	85.8	89.7	86.5	81.4	79.2	74.7	75.7	67.7
RMS (nm)	3.6	2.8	2.0	4.1	3.0	3.0	4.0	2.9	4.1	3.2	3.7	4.1	3.1	4.1	3.8	3.6
Waviness (nm)	0.1	0.3	0.2	0.3	1.5	1.5	2.5	1.4	2.6	1.7	2.2	2.6	1.6	2.6	2.3	2.1

Laser Power (W)	4.2	4.4	4.6	4.8	5	5.5	6	7	8	9	10	11	12	13	14	15
Film Thickness (nm)	75.2	66	77.1	55.5	72.2	60.2	53.2	46.6	41.8	35.9	27.3	25.6	22.4	22.9	25.3	19.6
RMS (nm)	6.5	6.7	5.5	7.2	9.8	7.9	7.2	3.5	4.1	3.6	3.5	3.3	3.3	3.0	2.8	2.4
Waviness (nm)	5.0	5.2	4.0	5.7	8.3	6.4	5.7	2.0	2.6	2.1	2.0	1.8	1.8	1.5	1.3	0.9

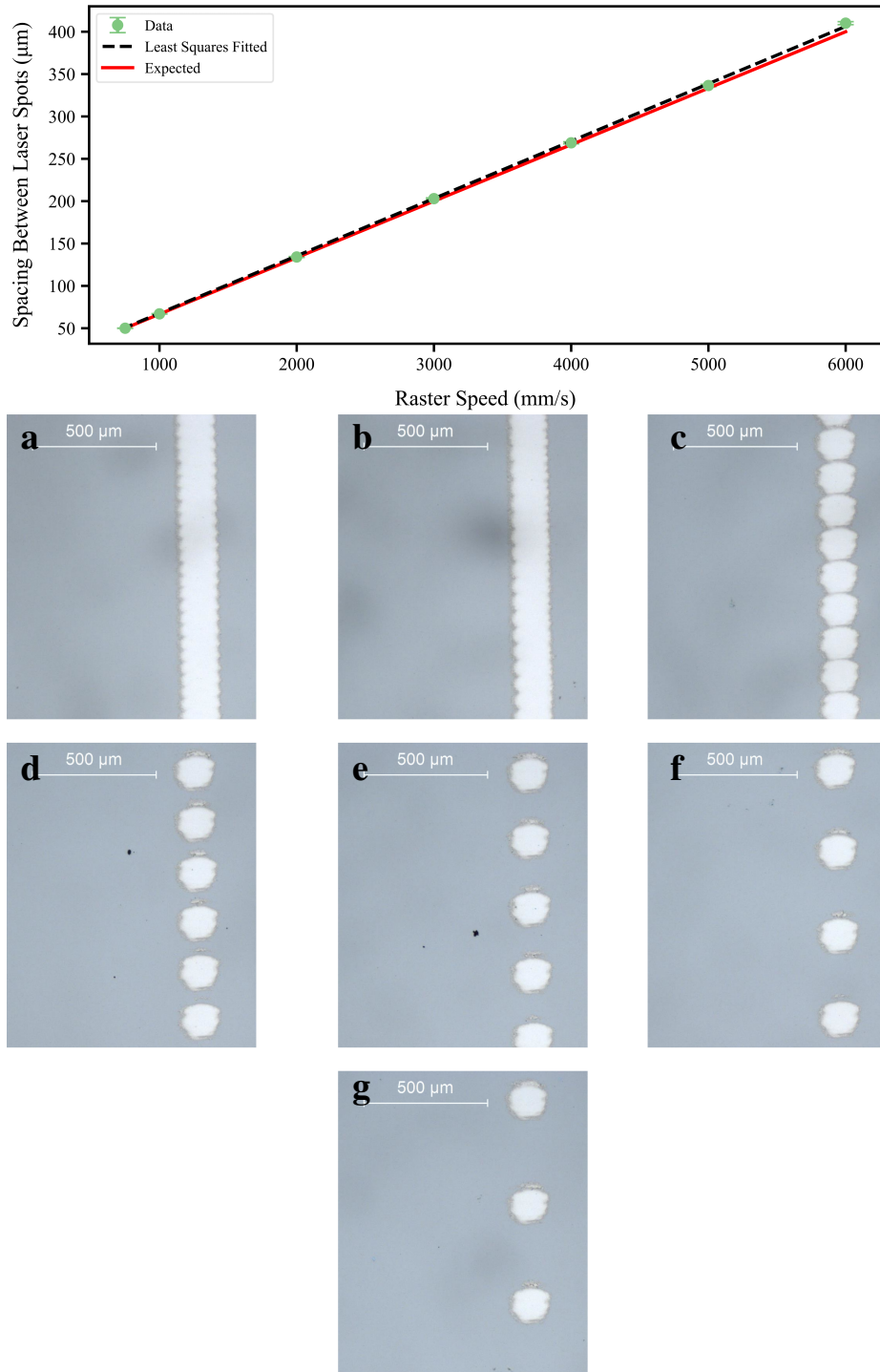


FIG. S3. Spacing between laser spots with increasing speed. The red line shows the expected spot spacing for the laser frequency of 15 kHz, dashed black shows the linear fitting of the data which yields a calculated laser frequency of 14.77 ± 0.04 kHz. Optical images **a-g** are examples of the images used to extract the distance using ImageJ, with the raster speeds of **a** 500 mm/s; **b** 1000 mm/s; **c** 2000 mm/s; **d** 3000 mm/s; **e** 4000 mm/s; **f** 5000 mm/s; **g** 6000 mm/s.

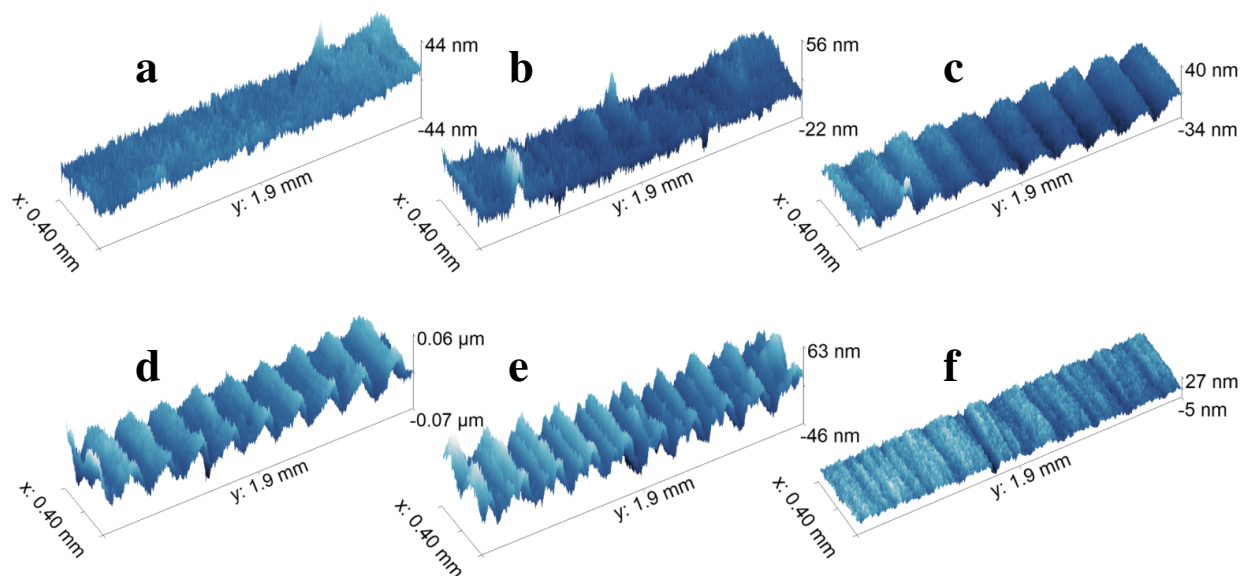


FIG. S4. Optical profilometry images of representative PEDOT:PSS samples after laser treatment, showing the onset of waviness caused by the laser, corresponding to the results of figure 3a of the main text. The laser powers shown are: **a** 0 W; **a** 3.2 W; **c** 3.6 W; **d** 4.2 W; **e** 5.5 W; **f** 15 W.

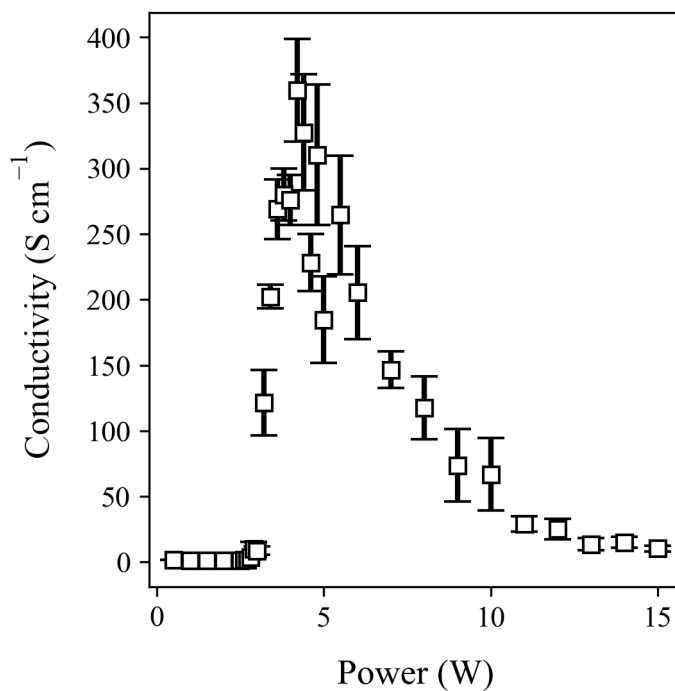


FIG. S5. Conductivity of PEDOT:PSS films with increasing laser power, calculated from the sheet resistance values of figure 2D and thickness values of figure 3A.

TABLE S2. Elemental position, fitted area, and atomic concentration from the fitting of the XPS data. Three measurements in different positions across laser treated and untreated samples are shown.

	Position [eV]												Si-O				
	C-(C,H)	C-S	C-O-C	C=O	(O) PSS	(O) PEDOT	OH _{ads}	Na	KLL	NH ₄ ⁺	NR ₄ ⁺	(S ²⁻) S 2p _{3/2}		PEDOT (S ²⁻) S 2p _{1/2}	PSS-Na ⁺ S 2p _{3/2}	PSSH S 2p _{3/2}	PSSH Na ⁺ S 2p _{1/2}
Untreated	284.8	285.8	286.7	287.6	531.8	533.3	534.6	536.2	402.1	164.1	165.2	168	169.1	168.6	169.7	1072.1	103.1
Untreated	284.8	285.8	286.6	287.6	531.9	533.3	534.7	536.1	402.2	164	165.2	168	169.1	168.6	169.7	1072.1	103
Untreated	284.8	285.8	286.7	287.7	531.8	533.4	534.6	536.2	402.2	164.1	165.2	168	169.1	168.6	169.7	1072.1	103.4
Average	284.8	285.8	286.7	287.6	531.8	533.3	534.6	536.2	402.2	164.1	165.2	168	169.1	168.6	169.7	1072.1	103.1667
Laser Treated	284.8	285.8	286.7	287.8	531.9	533.4	534.7	536.1	402.2	164	165.2	168	169.1	168.6	169.7	1072.1	103.3
Laser Treated	284.8	285.8	286.7	287.9	531.9	533.4	534.7	536	402	164	165.2	168.1	169.2	168.7	169.8	1072	103.4
Laser Treated	284.8	285.8	286.7	287.7	531.9	533.4	534.7	536.4	402.1	164	165.2	168	169.1	168.6	169.7	1072	102.2
Average	284.8	285.8	286.7	287.8	531.9	533.4	534.7	536.2	402.1	164	165.2	168.0	169.1	168.6	169.7	1072	103.0

	Raw Area												Ratio PEDOT/PSS Tot				
	C-(C,H)	C-S	C-O-C	C=O	(O) PSS	(O) PEDOT	OH _{ads}	Na	KLL	NH ₄ ⁺	NR ₄ ⁺	(S ²⁻) S 2p _{3/2}		PEDOT (S ²⁻) S 2p _{1/2}	PSS-Na ⁺ S 2p _{3/2}	PSSH S 2p _{3/2}	PSSH Na ⁺ S 2p _{1/2}
Untreated	2026.18	416.57	382.9	102.46	1928.97	1345.4	192.54	179.75	198.73	99.36	244.21	122.1	113.32	56.66	744.39	78.91	0.56
Untreated	2161.08	422.53	400.73	133.09	1836.07	1529.09	155.7	85.2	201.27	100.63	192.92	96.46	175.51	87.76	636.23	80.1	0.55
Untreated	2147.46	471.27	414.74	102.81	1875.11	1440.58	145.1	161.01	206.35	103.17	212.69	106.34	150.8	75.4	801.34	71.25	0.57
Average	2111.6	436.8	399.5	112.8	1880.1	1438.4	164.4	142	202.1	101.1	216.6	108.3	146.5	73.2	727.3	76.8	0.56
Laser Treated	2066.84	446.42	450.77	98.04	1850.88	1384.56	126.82	105.99	223.56	111.78	190.42	95.21	152.71	76.35	620.94	61.03	0.65
Laser Treated	2105.6	437.77	506.2	102.66	1744.78	1412.95	112.57	112.35	244.27	122.14	237.64	118.82	95.41	47.71	513.28	54.55	0.73
Laser Treated	2122.04	475.47	444.41	106.53	1956.67	1416.83	101.03	102.57	236.08	118.04	168.3	84.15	186.04	93.02	639.2	59.35	0.67
Average	2098.2	453.2	467.1	102.4	1850.8	1404.8	113.5	107	234.6	117.3	198.8	99.4	144.7	72.4	591.1	58.3	0.68

	Atomic Concentration [%]						Ratio PEDOT/PSS Tot							
	C-(C,H)	C-S	C-O-C	C=O	(O) PSS	(O) PEDOT		OH _{ads}	NH ₄ ⁺	NR ₄ ⁺	PEDOT (S ²⁻)	PSS-Na ⁺	PSSH	Na ⁺ PEDOT/PSS Tot
Untreated	39.7	8.17	7.51	2.01	14.69	10.26	1.47	2.07	3.3	3.3	4.06	1.89	3.13	0.55
Untreated	41.18	8.05	7.64	2.54	13.6	11.34	1.16	0.96	3.25	3.25	3.12	2.84	2.6	0.55
Untreated	40.41	8.87	7.81	1.94	13.72	10.55	1.06	1.78	3.29	3.29	3.39	2.41	3.24	0.57
Average	40.43	8.36	7.65	2.16	14.00	10.72	1.23	1.60	3.28	3.28	3.52	2.38	2.99	0.56
Laser Treated	40.4	8.73	8.82	1.92	14.07	10.53	0.97	1.22	3.7	3.7	3.16	2.54	2.61	0.65
Laser Treated	40.86	8.5	9.83	2	13.16	10.67	0.85	1.28	4.02	4.02	3.92	1.57	2.14	0.73
Laser Treated	40.29	9.03	8.44	2.03	14.45	10.47	0.75	1.15	3.8	3.8	2.71	3.0	2.61	0.67
Average	40.52	8.75	9.03	1.98	13.89	10.56	0.86	1.22	3.84	3.84	3.26	2.37	2.45	0.68

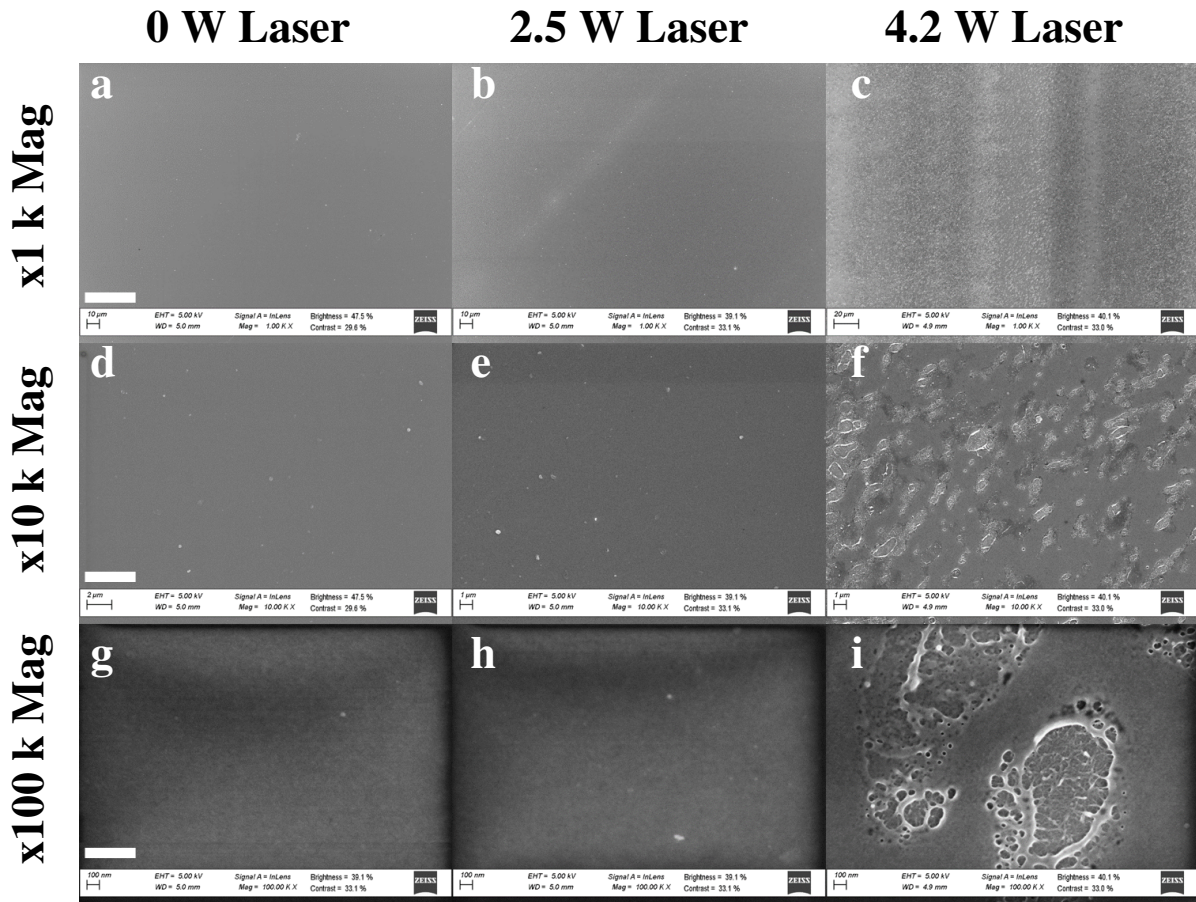


FIG. S6. SEM images of PEDOT:PSS films treated with **a, d, g** no laser, **b, e, h** 2.5 W laser, and **c, f, i** 4.2 W laser. The same area of material is shown for each laser power at **a-c** x1 k magnification, **d-f** x10 k magnification, and **g-i** x100 k magnification. White scale bars added to **a, d, g** are 50 μm , 5 μm , and 500 nm respectively.

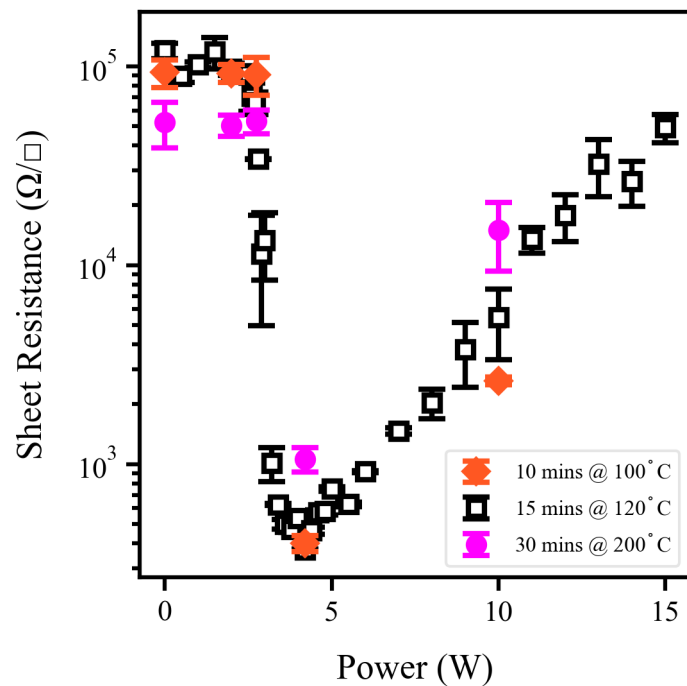


FIG. S7. Sheet resistance with increasing laser power for the standard curing process (black), high hydration films (cured for 10 minutes at 100°C, red), and low hydration films (cured for 30 minutes at 200°C, pink).

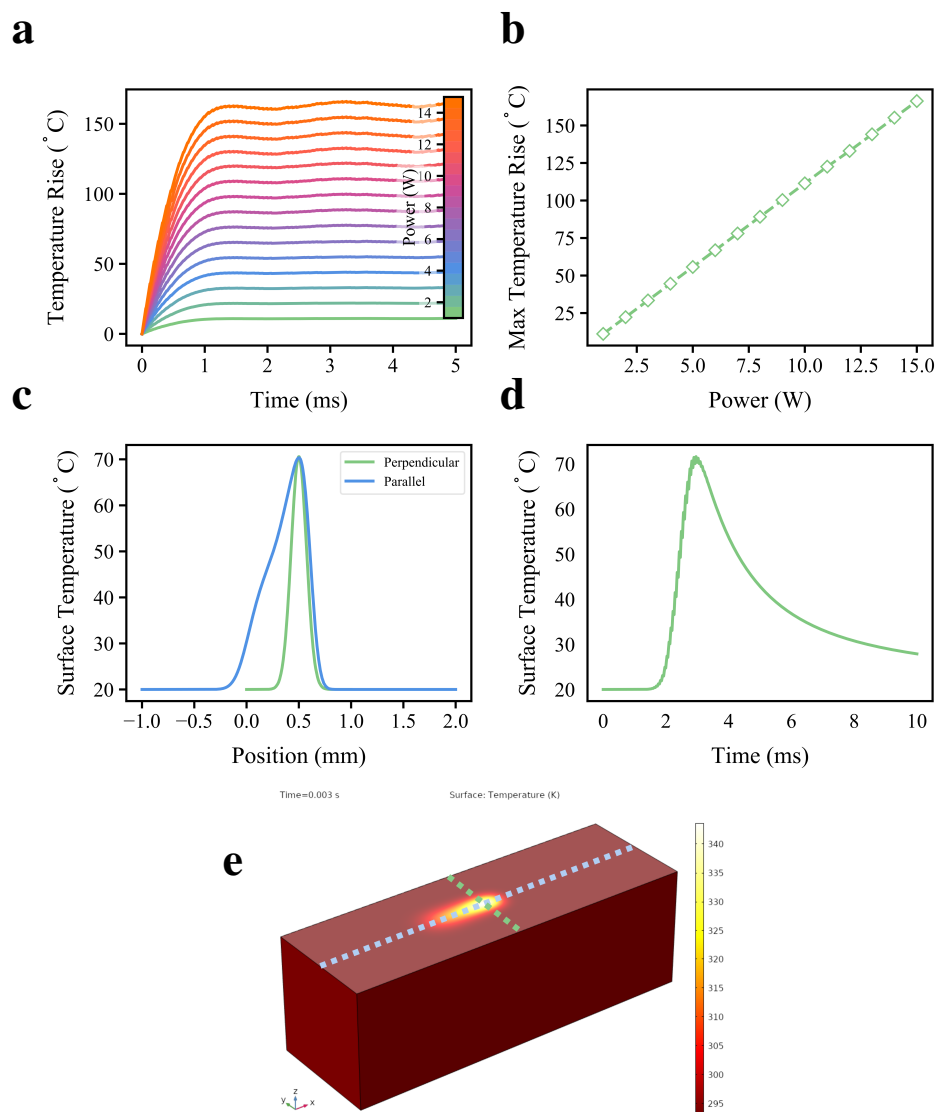


FIG. S8. Example outputs from COMSOL modelling of the laser interaction with PEDOT:PSS films. **a** Increase in maximum film temperature over 5 ms (the first 75 laser pulses) for increasing laser powers. **b** The maximum temperature increase over the simulation time for each laser power. **c** The temperature distribution perpendicular (green) and parallel (blue) to the direction of travel of the laser, shown for $t = 0.003$ s, the position of the cut lines in shown in the model of part **e**. FWHM discussed in the text are taken from this. **d** Temperature of a single point, and the intersection of the two cut lines in **e**, over 10 ms as the laser passes the spot. **e** 3D rendering of the absolute temperature at of the model at $t = 0.003$ s, overlaid with the cut lines referred to in parts **c** and **d**.

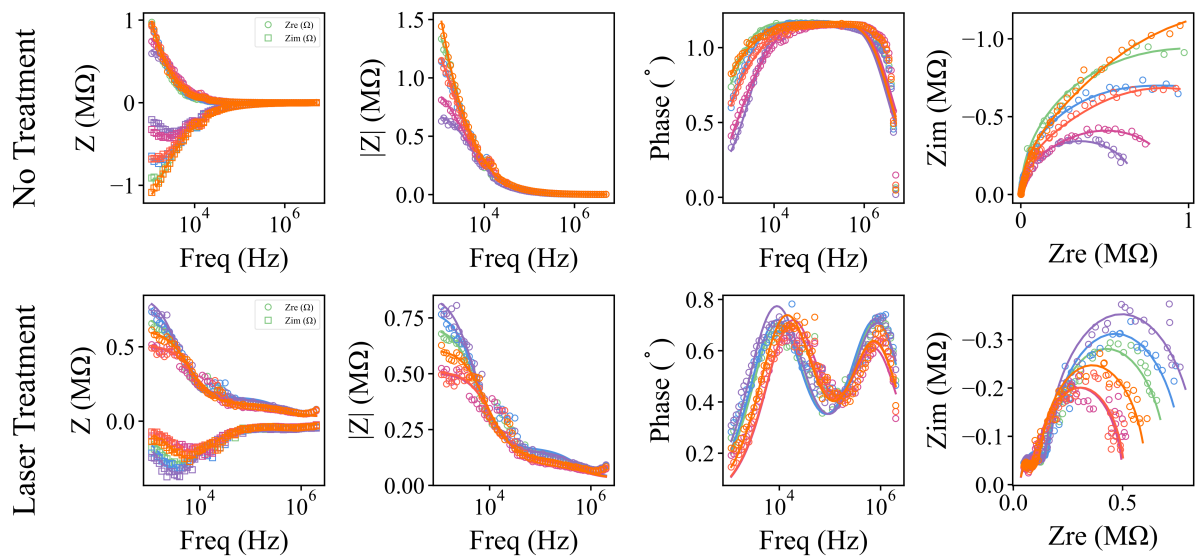


FIG. S9. Electrochemical Impedance Spectroscopy data for each untreated (top) and 4.2 W laser treated (bottom) PEDOT:PSS films. 6 measurements are fitted for treated and untreated material. Fitting was performed with a custom python script based on the equivalent circuit shown in figure 3j of the main text. The fitting algorithm gave equal weighting to each of the data representations shown here.

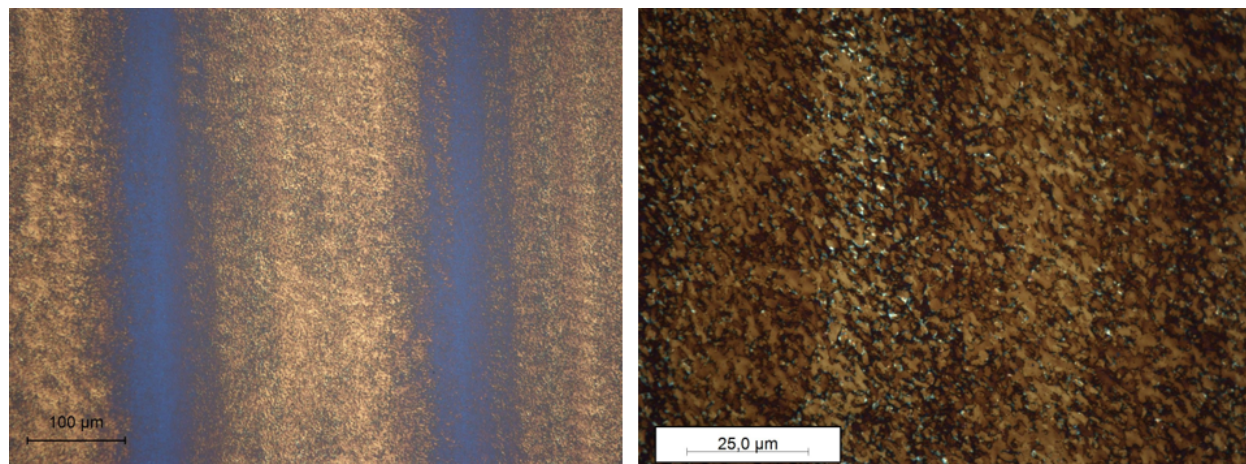


FIG. S10. Optical images of PEDOT:PSS films on ITO coated glass, after treatment with optimised laser parameters. The ITO layer (brown in the images) is significantly disrupted, and the PEDOT:PSS layer (blue in the images) appears very different from the standard process on glass slides. These effects make ITO coated glass an unsuitable substrate for CAFM measurements of this process.

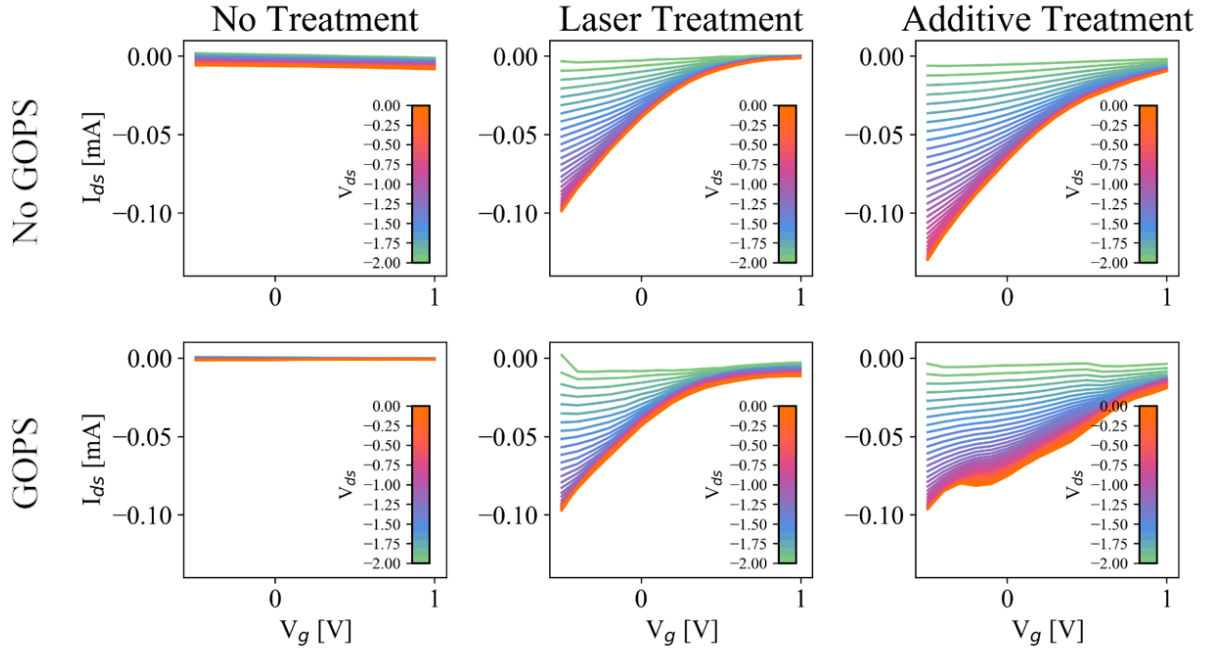


FIG. S11. Transfer characteristics of the same OEFT devices as displayed in figure 4 of the main text.

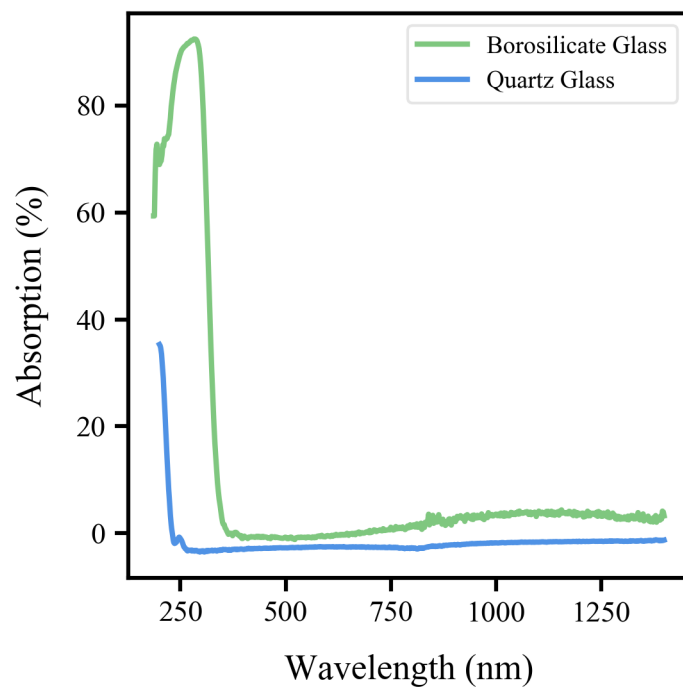


FIG. S12. UV-vis absorption spectra for standard borosilicate float glass and fused quartz glass. Quartz is used as the substrate for UV-vis measurements of the PEDOT:PSS as the borosilicate would obscure the PSS absorption peak seen in figure 3c.